

## Article

# Solar Chimneys as an Effective Ventilation Strategy in Multi-Storey Public Housing in the Post-COVID-19 Era

Pau Chung Leng <sup>1,\*</sup>, Siew Bee Aw <sup>1</sup>, Nor Eeda Haji Ali <sup>2</sup>, Gabriel Hoh Teck Ling <sup>1,\*</sup>, Yoke Lai Lee <sup>1</sup> and Mohd Hamdan Ahmad <sup>1</sup>

<sup>1</sup> Faculty of Built Environment and Surveying, Universiti Teknologi Malaysia, Skudai 81300, Johor, Malaysia; awsiewbee@gmail.com (S.B.A.); lylai@utm.my (Y.L.L.); b-hamdan@utm.my (M.H.A.)

<sup>2</sup> Faculty of Architecture, Planning & Surveying, Universiti Teknologi MARA Perak Branch, Seri Iskandar 32610, Perak, Malaysia; noree038@uitm.edu.my

\* Correspondence: pcleng2@utm.my (P.C.L.); gabriel.ling@utm.my (G.H.T.L.)

**Abstract:** This paper studies the effectiveness of a solar chimney for improving ventilation and air-exchange rates in multi-storey public housing in tropical climates for the potential mitigation of airborne disease transmission. Virtual models of a typical apartment room with natural cross-ventilation, replicated across four levels to mimic a multi-storey block, were set up with six internal wind velocity sensor points per floor. The simulation software Energy2D was then used to evaluate the performance of the models, first testing the presence of a solar chimney, and then additionally the degree to which the solar chimney model was affected by a complementary ceiling fan. Wind velocity was also measured, as this is a variable that affects ACH rates. Using a non-parametric Wilcoxon signed-rank test, the introduction of a solar chimney was found to have a significant impact on air-flow rates (a variable that positively affects air-exchange rates), resulting in a *p*-value of 0.000 and *Z*-value of  $-3.920$ . Regression analysis determined that the solar chimney's effect was enhanced when complemented by a ceiling fan (R-squared value of 0.4687). Consequently, we propose several design strategies that may enable the adoption of the solar chimney concept to improve natural ventilation in residential units.

**Keywords:** solar chimney; natural ventilation; air-exchange rate; multi-storey housing; tropical climate



**Citation:** Leng, P.C.; Aw, S.B.; Ali, N.E.H.; Ling, G.H.T.; Lee, Y.L.; Ahmad, M.H. Solar Chimneys as an Effective Ventilation Strategy in Multi-Storey Public Housing in the Post-COVID-19 Era. *Buildings* **2022**, *12*, 820. <https://doi.org/10.3390/buildings12060820>

Academic Editor: Dirk H.R. Spennemann

Received: 22 April 2022

Accepted: 1 June 2022

Published: 13 June 2022

**Publisher's Note:** MDPI stays neutral with regard to jurisdictional claims in published maps and institutional affiliations.



**Copyright:** © 2022 by the authors. Licensee MDPI, Basel, Switzerland. This article is an open access article distributed under the terms and conditions of the Creative Commons Attribution (CC BY) license (<https://creativecommons.org/licenses/by/4.0/>).

## 1. Introduction

The Spanish flu pandemic in 1918 and, more recently, the global COVID-19 pandemic, serve to highlight the importance of air circulation for the mitigation of airborne contagious diseases—especially in high-density living environments. The inflow of fresh, outdoor air helps to minimise the accumulation of virus particles in indoor spaces [1]. Epidemiological data show a much higher incidence of COVID-19 in developed European countries—such as Slovenia—and North American countries during the autumn and winter seasons than in African or Asian countries, which have milder climates that allow people to spend more time outdoors, where airborne spread is less significant [2].

According to the World Health Organization, airborne viruses spread in poorly ventilated or crowded indoor spaces, as aerosols can remain airborne and travel within such confined settings. As modern building façades use more glazing and fixed glass panels, indoor air circulation is assisted by heating, ventilation, and air conditioning (HVAC) systems or air conditioning mechanical ventilation (ACMV) systems in countries that do not require heating [3].

Despite the acknowledgement of the importance of good air circulation, there are limited references for specific ventilation and filtration targets beyond a need to increase the air-exchange rate, especially in multi-storey buildings in the tropics [4,5]. This paper assesses the current ventilation performance of a multi-storey residential building in

Malaysia and, through virtual simulations, explores the effectiveness of the concept of a solar chimney to promote natural ventilation for the aforementioned building typology.

The American Society of Heating, Refrigerating, and Air-Conditioning Engineers (ASHRAE) has established ventilation guidelines for most interior environments [6]. However, these guidelines are meant to achieve basic levels of acceptable indoor air quality, rather than passive infection control [7]. This is achieved by encouraging the air-exchange rate in a space, commonly expressed in units of air changes per hour (ACH), although it can also be measured as total volumetric flow, volumetric flow per person and area, or outdoor air ventilation rates [8].

The formula for calculating ACH is expressed as follows:

$$\text{ACH} = 3600 \times Q / \text{Vol} \quad (1)$$

where ACH = air changes per hour, measured in cu.m/h; Q = volumetric flow rate, in cu.m/s, derived from air-flow velocity (m/s)  $\times$  cross-sectional area (sqm); and Vol = the volume of the space, in cu.m.

Notwithstanding factors such as wind effect ventilation, buoyancy effect, and loss coefficient, which may affect the velocity of natural ventilation, an increase in air-flow velocity (measured in m/s) increases the volumetric flow rate in a fixed space which, in turn, increases the achievable ACH rate.

According to ASHRAE Standard 62.1-2019, a single-family home with three bedrooms, a default occupancy of 213.77 m<sup>2</sup> (2301 sqft), and 2.4 m (8 ft) spatial height is recommended to have an ACH rate of at least 4.0–6.0 ACH, or 0.32–0.35 ACH per person [6,8]. Fisk [9] highlighted the effectiveness of higher ACH rates as an infection control mechanism, in line with ASHRAE's minimum ACH recommendations for public buildings such as hospitals, at almost 10 times more than the recommendations for residential use.

In Malaysia, the ACH recommendations in the Third Schedule of the Uniform Building By-Laws 1986 (Amendment 2012) (UBBL) are concerned primarily with fresh air ventilation in spaces that are windowless and without access to external walls or fenestrations. Such habitable rooms should have a minimum fresh air change rate of 0.28 cmm, or 16.8 cmh per person, while bathrooms and toilets should have either 0.61 cmm per square metre or 10 ACH (whichever is lower) [10]. The UBBL do not include ACH recommendations for naturally ventilated spaces.

There are several passive strategies to promote natural ventilation in indoor environments, including atria, courtyards, and solar chimneys, the latter of which are the focus of this paper. Solar chimneys are typically utilised on southwest- and south-facing buildings for the purposes of ventilation, heat insulation, and/or heat preservation, depending on the underlying intent of the designer. A solar chimney uses the thermal pressure differentiation between indoor and outdoor spaces to generate natural airflow [11]. When the external wall of the solar chimney is heated by the sun, the air density within the solar chimney drops. Air is sucked up through a low opening on the internal wall and expelled from an opening high on the external wall.

Various studies have been conducted to determine the efficiency of the Trombe wall—a type of solar chimney—using field measurements or software simulations [12,13]. This includes research by Du et al., who studied the effectiveness of the Trombe wall by integrating mathematics and modelling to predict, derive, and examine patterns of air velocity [11]. Solar chimneys drive airflow through thermal buoyancy; by maximising solar gain on its external façade, the chimney acts as a thermo-syphoning air channel to draw indoor air out of the building [14].

However, while solar chimneys have been relatively well researched in Western countries, research on their effectiveness in tropical climates is still nascent. Previous studies on solar chimneys have tended to focus on industrial buildings, singular buildings such as residential homes, or large public buildings [15,16]. Tan and Wong [15] determined that a solar chimney was able to naturally improve interior air speed and expedite changes in air temperature when tested in a single-storey classroom in Singapore. Hassanein and

Abdel-Fadeel [17] found that the use of multiple solar chimneys, oriented in different directions, further improves air-flow rates and reduces indoor temperatures, although their effectiveness is greatest when directly facing the sun. A quicker passive reduction in indoor temperature reduces the need and the time required for cooling demand. Furthermore, Gong et al. [18] determined that users in tropical climates can accept air velocity rates ranging from 0.3 m/s to 0.9 m/s, while Roghanchi et al. [19] ascertained that 1.0–2.0 m/s is ideal for thermal comfort.

This paper therefore focuses on two research gaps in solar chimney studies: their effectiveness in improving interior air speed and circulation in tropical climates, and their application in multi-storey public housing, where the addition of such a substantial element may incur critical cost implications.

Firstly, we propose that solar chimneys can be an effective passive method to improve natural ventilation in tropical buildings. By achieving the above objective, the findings of this study are not only beneficial from an architectural standpoint, but also advantageous for future health policies, as improved fresh outdoor air circulation in multi-storey housing may potentially slow down the spread of airborne contagious diseases.

The remainder of the paper is structured as follows: Section 2 presents the methodology covering field measurements, coupled with validation of the Energy2D software, followed by a simulation of four scenarios; Section 3 presents the results and discussions of the simulated scenarios; finally, Section 4 provides our conclusions and recommendations.

As a passive method to accelerate ACH, increase fresh air inflow, and displace airborne contaminants, it is hoped that a more widespread acknowledgement and adoption of this strategy may limit the impact of future airborne diseases, such as the SARS-CoV-2 virus.

## 2. Methodology

### 2.1. Case Study

A four-storey public housing development in Taman Pulai Flora, Skudai, Johor, Malaysia, was selected to study the ventilation performance of typical multi-storey residential buildings in a tropical climate. Details of the development are included in Table 1.

**Table 1.** Case study building.

Parameters	Description/Value
Physical Program	3 blocks of 4–5 storey mid–low-cost apartments
Coordinates	1°33′01.29″ N, 103°37′20.30″ E
Selected Block	Block B
Orientation of Selected Case Study Block	182° (South)
Unit Layout	975 sqft, 3-bedroom unit with kitchen and utility space
Type of Roofing	Clay roof tiles
Outdoor Air temperature	30 °C
Outdoor Wind Velocity	1.0 m/s (constant)
Shading System	Not available

A typical apartment unit is approximately 975 sqft, with 3 bedrooms (a master bedroom with an attached bathroom, and two normal bedrooms), an open living and dining space, a kitchen, and a utility room. A unit on Level 3 of Block B became the case study (see Figure 1). The orientation of the unit was such that it faced south, along the front façade of the building (see Figure 2). The south-facing openings served as air-flow inlets, while the air-flow outlets faced north. The illustrated diagram of the master bedroom with attached bathroom is shown in Figure 3.



**Figure 1.** Location plan of the case study building, as seen from Google Earth.



**Figure 2.** Front and rear façade of the test room. ((left): front façade of the case study building/inlet window; (right): rear façade of the case study building/the washroom exterior façade/outlet window).

In order to study the performance of the solar chimney, the master bedroom was chosen for simulation modelling and analysis, as it had direct access to both north- and south-facing openings by virtue of its attached bathroom (see Figure 4). The bathroom served as a solar chimney for the master bedroom. Details of the case study room are included in Table 2.





**Figure 3.** Plan view of the modelled case study room (master bedroom with attached bathroom).

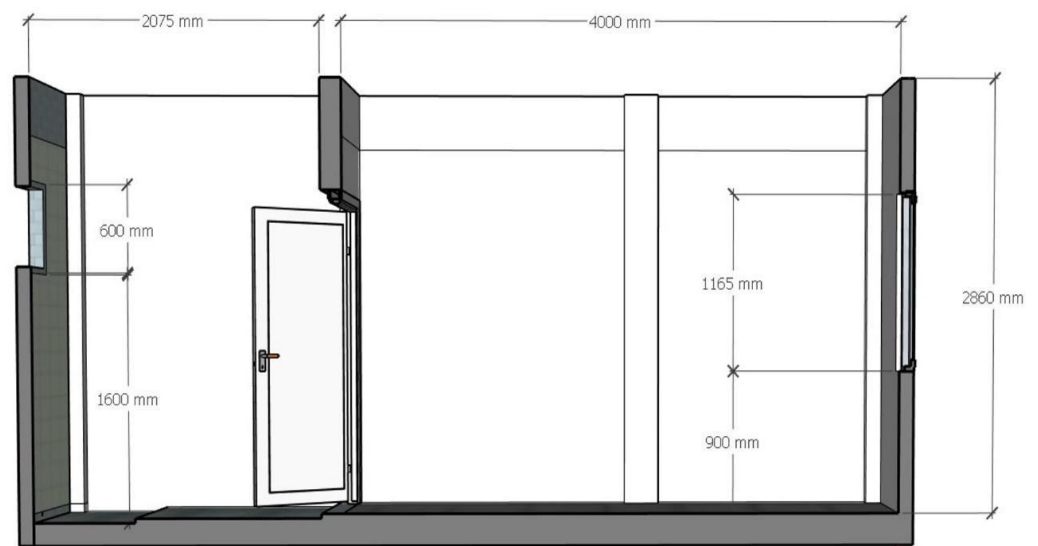


**Figure 4.** Section across the modelled master bedroom and attached bathroom.

## 2.2. Field Measurements and Software Validation

### 2.2.1. Field Measurements

Field measurements were conducted for 8 full days between 26 March 2022 and 2 April 2022 in the selected case study unit, which was located on Level 3 in Block B. The field measurements were carried out for at least 1 week to sufficiently cover variations in climatic conditions in Malaysia, which is hot and humid throughout the year. The indoor air velocity (m/s) of the bedroom was recorded with a single-probe Delta Ohm HD31.1 Portable Multifunction Instrument and Data Logger, which has a measuring accuracy of  $\pm 0.02\%$  (excluding probe-related errors) at 20 °C. The data logger was set up in the middle of the room at 1.5 m above the floor level and 1.8 m away from the external-facing window of the room, as illustrated in Figures 5 and 6. The corresponding software, installed on a personal computer, was used to set the data logger to read measurements at 5-min intervals.

**Table 2.** Description of the case study room (master bedroom with attached bathroom).

Parameters	Master Bedroom	Bathroom
Location	Level 3	Level 3
Dimensions	Max. 4 m (L) × 2.825 m (W) × 2.86 (H)	2.075 m (L) × 1.35 m (W) × 2.86 m (H)
Area (sqm)	10.3 sqm	2.8 sqm
Volume (cu.m)	29.458 cu.m	8.008 cu.m
Air-Flow Direction	Inlet	Outlet
Opening Orientation	South	North
Opening Size	1.8 m × 1.165 m (2.097 sqm) with sill height 900 mm above floor level	0.6 m × 0.6 m (0.36 sqm) with sill height 1.6 m above floor level
Glazing Type	Single-layer clear glazing (untinted)	Single-layer clear glazing (untinted)
Assumed Window Opening Position	100% opened	100% opened
Wall–Window Ratio (WWR)	38%	38%
Type of Wall	115 mm thick brick wall with plastering on both sides	115 mm thick brick wall with plastering on external side and wall tiles on internal side
Type of Ventilation	Natural ventilation with ceiling fan	Natural ventilation via window
Cross-Ventilation	Yes (when bathroom door is kept open)	

**Figure 5.** AP471S wind velocity hotwire airspeed probes [14] (left), and setup of field measurements (right).

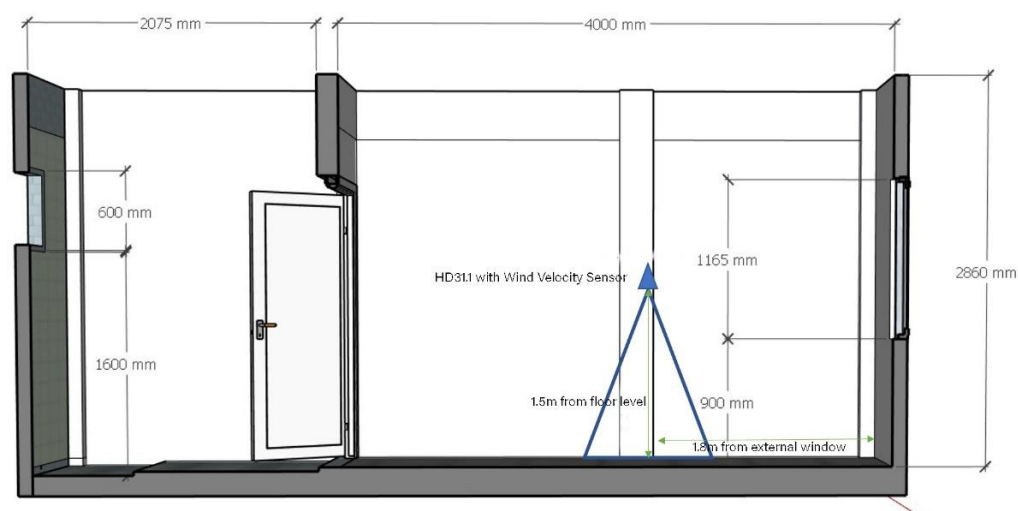


**Figure 6.** Position of the wind velocity sensor in the case study room (master bedroom in a Level 3 apartment unit).

The results of the field measurements are shown in Figure 7. The results from the initial set-up day on 25 March 2022 were disregarded, as the recordings only commenced in the evening. The average wind velocity measured in the case study unit was 0.019 m/s, with a range of 0–1.1 m/s. Based on the recorded data, 69.56% of the total field measurements recorded 0 m/s. The wind velocity exceeded 1 m/s only thrice—at 14:44 and 14:29 on 27 March 2022, and also at 14:34 on 28 March 2022—due to increased wind flow during rainy periods. This represented 0.13% of the measured duration.

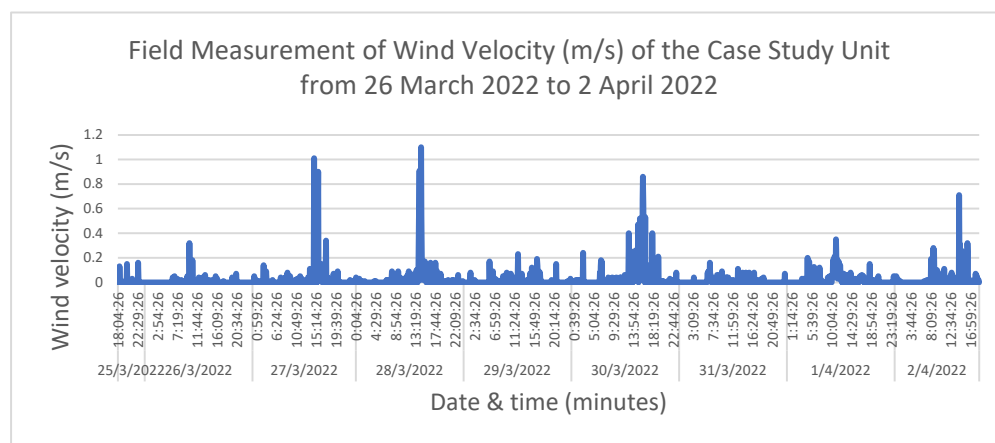


**Figure 7.** Field measurement results of the indoor wind velocity (m/s), taken at 5-min intervals.

Out of the 2314 recorded data values logged during the 8 days, there were only 39 instances detected of wind velocity exceeding 0.2 m/s, and 17 instances of wind velocity exceeding 0.4 m/s. Therefore, it can be inferred that the indoor airflow was poor, and the probability of the air velocity exceeding 1.0 m/s in the current case study unit's layout, without the aid of fans, was very low.

### 2.2.2. Software Validation

The field measurement results were also used to validate the Energy2D [20] simulation software for its ability to simulate wind velocity in tropical environments. Energy2D was used to conduct a theoretical evaluation of solar-induced ventilation in this study. This software has already been used to conduct simulations for research, and is widely recommended in the previous literature [21–23].

This study evaluated natural ventilation in two ways: firstly, by determining the average air velocity along the horizontal plane in the case study room and the solar chimney space (attached bathroom), illustrated in section view; and secondly, by determining the ACH rate, which calculates all velocity vectors that pass through apertures into an indoor space.

The master bedroom of the case study unit was modelled and then imported into Energy2D. Wind velocity sensors were located at the centre of the bedroom on each level of the apartment block, as illustrated in Figure 8. The settings used in Energy2D were as described in Table 3.

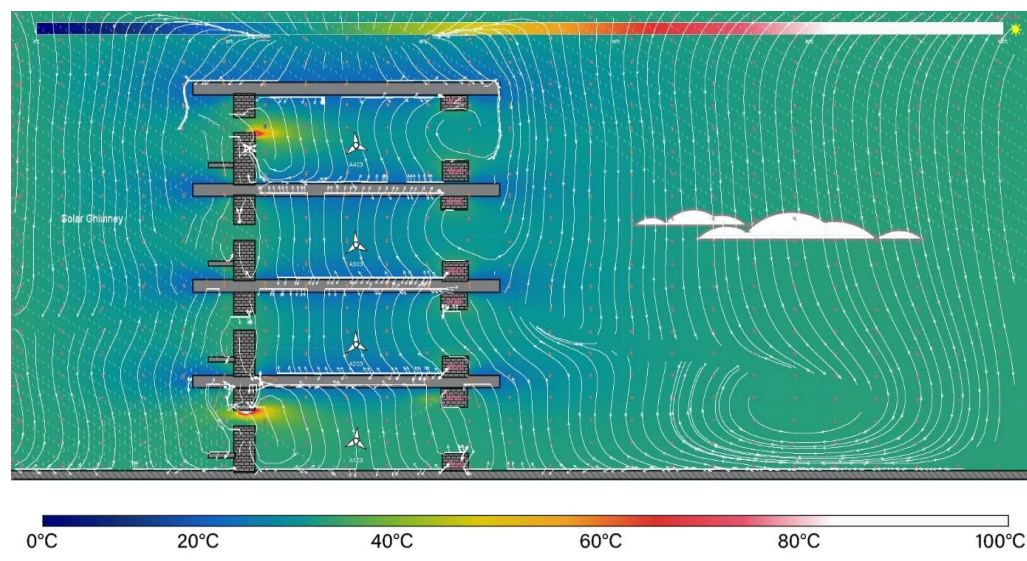


**Figure 8.** A sectional view of the simulation setup in Energy2D. The results of Sensor A3C3 (Level 3 simulation) were compared against the field measurements shown in Section 2.2.1.

The comparisons between the field measurements and simulation results were made through the Pearson's correlation coefficient, root-mean-square error (RMSE), and mean bias error (MBE), using the equations shown below. The  $r$  coefficient was used to determine the correlation between two groups of measured values from the field measurements and simulated results. A direct relationship is stronger when the R-value is close to 1 or  $-1$ , which were the highest values from both datasets. The RMSE reveals the degree of spread within the sample set. Finally, the MBE indicates how well the sample is predicted, and whether the model is over- or underestimated.

Although the feasibility of RMSE and MBE is not governed by any guidelines, both have been extensively used by researchers to calibrate study processes and compare simulated and field measurement results [24–26].

Pearson's correlation coefficient, RMSE, and MBE were calculated using Equations (2)–(4), respectively.

$$r = (n(\sum(xy) - (\sum x)(\sum y)) / \sqrt{([n\sum x^2 - (\sum x)^2][n\sum y^2 - (\sum y)^2]}) \quad (2)$$

$$\text{RMSE} = \sqrt{((\sum x - y)^2) / n} \quad (3)$$

$$\text{MBE} = \frac{\sum (x - y)}{n} \quad (4)$$

where  $y$  = the simulation-generated value,  $x$  = the measured value from field measurements, and  $n$  = the total number of measurements.



**Table 3.** Properties settings for the simulation in Energy2D.

<b>Medium Settings</b>	
Background Temperature	30 °C
Conductivity	0.026341001 W/(m °C)
Specific Heat	1.006500006 J/(kg °C)
Density	1.164899945 kg/m <sup>3</sup>
<b>General Settings</b>	
Convective	Yes
Sunny	Yes
Time-step Length	0.1
With × Height	20 × 30 m
<b>Sunlight Settings</b>	
Sun Angle	130°
Solar Power Density	1000 W/m <sup>3</sup>
<b>Thermal Boundary Settings</b>	
Thermal Boundary Condition	Dirichlet (constant temperature)
Upper Boundary Temperature	30 °C
Right Boundary Temperature	30 °C
Lower Boundary Temperature	15 °C
Left Boundary Temperature	30 °C

The summary of the comparison of results between the simulated and field measurements is tabulated in Table 4. The R-value obtained ranged between 0.123 and 0.647. Although the R-value seemed to indicate a weak correlation due to differences in the total decimal values recorded from the field measurement data (2 decimal points) and the simulation data (4 decimal points), the wind velocity was considered consistent, as both scenarios achieved nearly static air movement rates—almost 0 m/s—as well as a significant result based on Pearson’s correlation coefficient. Overall, the Pearson’s correlation between the variables indicated a positive relationship between both sets of data.

**Table 4.** Comparison between field measurements and computer-simulated results.

Date	Time (Hour)	Pearson’s Correlation (R-Value)	RMSE	MBE
25 March 2022	1800	0.364	0.046	0.020
	1900	0.331	0.011	0.003
	2000	0.647	0.043	0.013
	2100	0.303	0.009	0.002
	2200	0.335	0.046	0.013
	2300	0.349	0.103	0.059
26 March 2022	0000	0.123	0.113	0.054
	0100	0.167	0.155	0.075
	0200	0.236	0.155	0.075

**Table 4.** *Cont.*

Date	Time (Hour)	Pearson's Correlation (R-Value)	RMSE	MBE
	0300	0.167	0.158	0.066
	0400	0.181	0.108	0.05
	0500	0.158	0.119	0.058
	0600	0.2801	0.027	0.02
	0700	0.1287	0.009	0.004
	0800	0.4466	0.007	0.003
	0900	0.5093	0.094	0.034
	1000	0.2309	0.052	0.018
	1100	0.163	0.108	0.05
	1200	0.169	0.093	0.04
	1300	0.383	0.108	0.053
	1400	0.198	0.104	0.042
	1500	0.142	0.193	0.108
	1600	0.529	0.171	0.075
	1700	0.1795	0.158	0.083
	1800	0.16	0.091	0.033

The RMSE results ranged between 0.007 and 0.193, while MBE revealed low error values (0.003–0.108) and a significant correlation coefficient, indicating a high level of importance. Therefore, the results of the simulations produced using Energy2D for tropical climates were considered to be reliable and consistent with the actual onsite environment [27].

### 3. Results and Discussion: Scenario Simulations

Four different scenarios were simulated in Energy2D, varying in the presence of a solar chimney (SC), ceiling fan, and an aperture design that allows airflow. In all scenarios, the bathroom-cum-solar-chimney was positioned on the leeward side, and the inlet aperture in the bedroom was positioned on the windward side. The scenarios are summarised in Table 5.

**Table 5.** Summary of four simulated scenarios based on opening type, presence of solar chimney elements, and presence of a ceiling fan.

	Scenario 1	Scenario 2	Scenario 3	Scenario 4
Description	Bathroom with 0.6 m × 0.6 m window at 1.6 m sill height		Bathroom with 2.7 m height internal wall and full-height external wall	
Solar Chimney	No	No	Yes (external wall acts as a solar chimney element)	
Ceiling Fan	No	Yes (consistently 3 m/s)		Yes (consistently 3 m/s)
Outdoor Wind Source	1 m/s (consistent)			

All four bedroom and bathroom scenarios were modelled and then replicated on four levels, to mimic the typical repetitive section of an apartment building. Eight wind velocity sensors were then positioned on every level, yielding a total of thirty-two sensors. At each level, two sensors were located outside the building model, on the windward and leeward sides, respectively, while another six were distributed across the bedroom and the

bathroom-cum-solar-chimney, as illustrated in Figure 9. The results of the simulations were as shown in Figure 10.

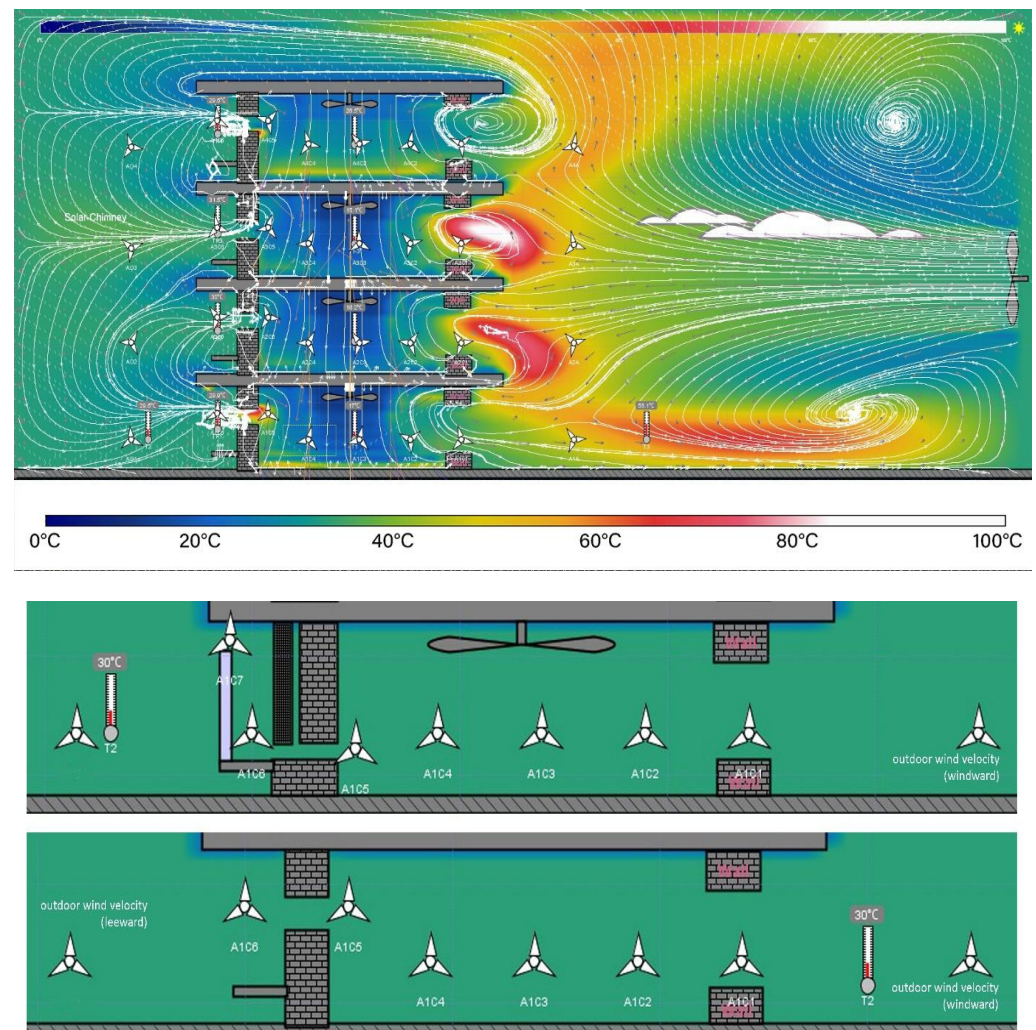
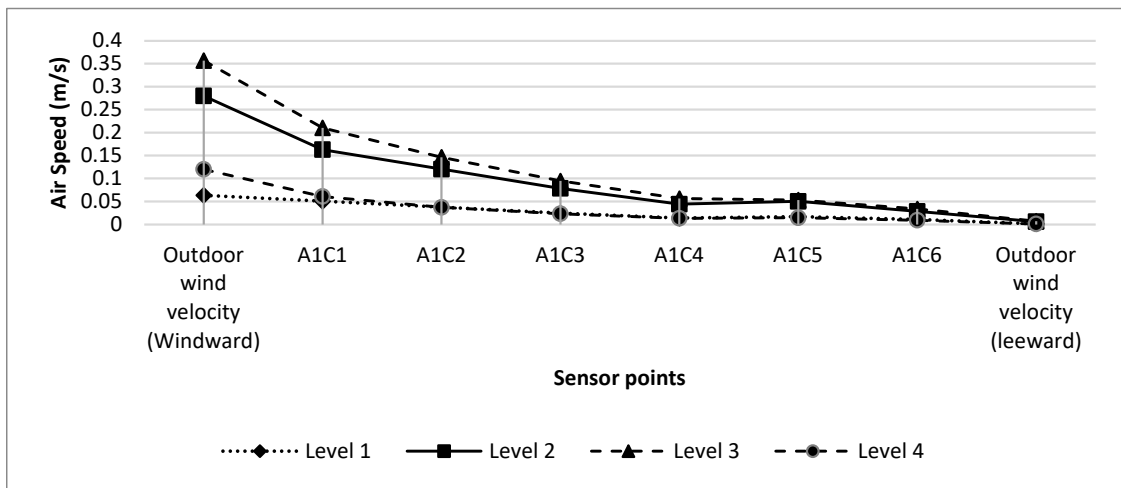


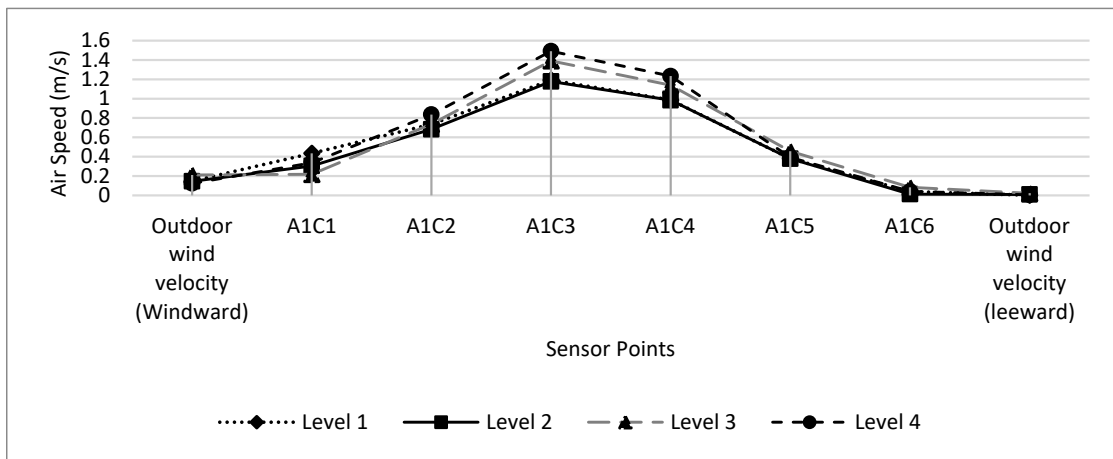
**Figure 9.** Locations of wind velocity sensors in each simulation model, with SC (middle) and without SC (below).

The means of the scenarios with solar chimneys (Scenarios 3 and 4) indicated positive improvements in air velocity within the room in comparison with scenarios without solar chimneys (Scenarios 1 and 2), as described in Table 6. The results measured on Level 3 exhibited the greatest increase in the mean, from 1.392 to 1.427.

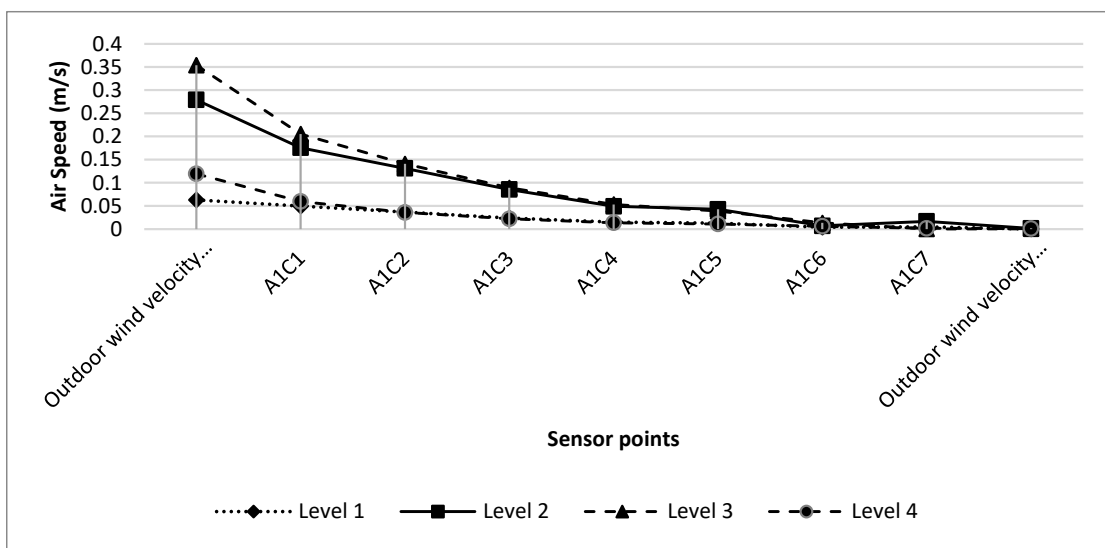
The Wilcoxon signed-rank test was conducted to ascertain the degree of impact the induction of a solar chimney effect has on air velocity. As described in Tables 6 and 7, the Wilcoxon signed-rank test of the SC and non-SC options based on 20 data points (amounting to 200 s of observation) revealed that the installation of the SC elicited a significant positive change in air speed across all levels of the simulated apartment, with a Z-value of  $-3.920$  and a  $p$ -value of 0.000 (refer Table 8). The results were further analysed via a regression model to determine whether SC effectiveness could be affected by the presence of a ceiling fan, which provides a constant means to direct the airflow within the space.



(a)



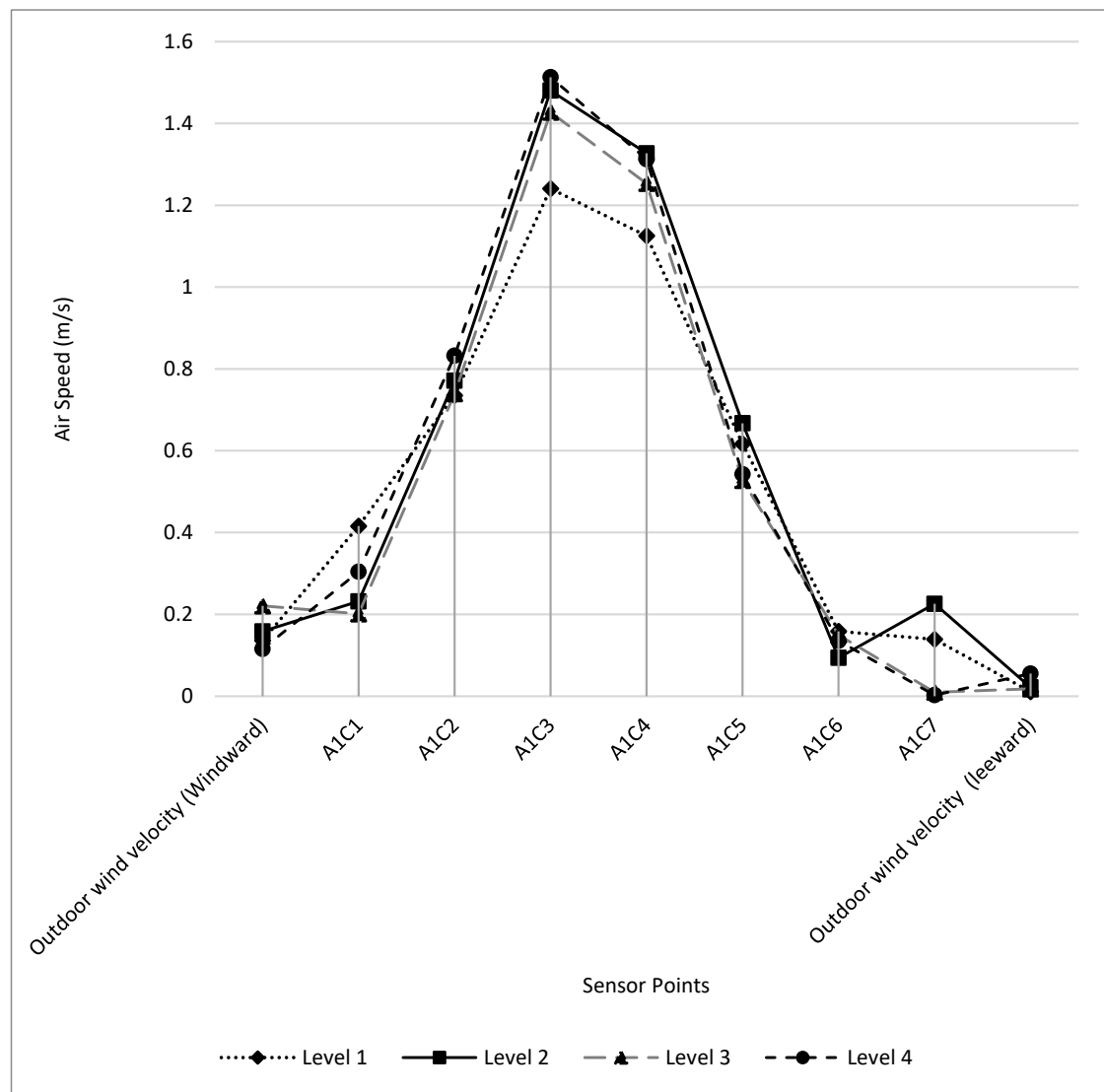
(b)



(c)

Figure 10. Cont.





(d)

**Figure 10.** Simulation results for all 4 scenarios: (a) Scenario 1, (b) Scenario 2, (c) Scenario 3, (d) Scenario 4.**Table 6.** The mean and standard deviation in the air velocities measured across all 4 simulated scenarios.

Descriptive Statistics					
	<i>n</i>	Mean	Std. Deviation	Minimum	Maximum
Lv1_WSC2	20	1.1926711850	0.00004079415	1.19254920	1.19272670
LV2_WSC2	20	1.1786533300	0.00028823077	1.17852620	1.17980440
LV3_WSC2	20	1.3918028400	0.00086532815	1.39152810	1.39540420
LV4_WSC2	20	1.4909670350	0.00013830683	1.49091960	1.49155140
Lv1_SC2	20	1.2408699950	0.00005342968	1.24068400	1.24090390
LV2_SC2	20	1.4806610100	0.00017530665	1.48057120	1.48122070
LV3_SC2	20	1.4273691850	0.00067709360	1.42715330	1.43018340
LV4_SC2	20	1.5131995450	0.00009076602	1.51316340	1.51357600

Note: SC = with solar chimney, WSC = without solar chimney.

**Table 7.** Mean and total ranks of the 20 data points used to conduct the Wilcoxon signed-rank test.

		Ranks		
		<i>n</i>	Mean Rank	Sum of Ranks
Lv1_SC2–Lv1_WSC2	Negative ranks	0 <sup>a</sup>	0.00	0.00
	Positive ranks	20 <sup>b</sup>	10.50	210.00
	Ties	0 <sup>c</sup>		
	Total	20		
LV2_SC2–LV2_WSC2	Negative ranks	0 <sup>d</sup>	0.00	0.00
	Positive ranks	20 <sup>e</sup>	10.50	210.00
	Ties	0 <sup>f</sup>		
	Total	20		
LV3_SC2–LV3_WSC2	Negative ranks	0 <sup>g</sup>	0.00	0.00
	Positive ranks	20 <sup>h</sup>	10.50	210.00
	Ties	0 <sup>i</sup>		
	Total	20		
LV4_SC2–LV4_WSC2	Negative ranks	0 <sup>j</sup>	0.00	0.00
	Positive ranks	20 <sup>k</sup>	10.50	210.00
	Ties	0 <sup>l</sup>		
	Total	20		

Note: SC = scenarios with solar chimney, WSC = scenarios without solar chimney. <sup>a</sup> Lv1\_SC2 < Lv1\_WSC2; <sup>b</sup> Lv1\_SC2 > Lv1\_WSC2; <sup>c</sup> Lv1\_SC2 = Lv1\_WSC2; <sup>d</sup> LV2\_SC2 < LV2\_WSC2; <sup>e</sup> LV2\_SC2 > LV2\_WSC2; <sup>f</sup> LV2\_SC2 = LV2\_WSC2; <sup>g</sup> LV3\_SC2 < LV3\_WSC2; <sup>h</sup> LV3\_SC2 > LV3\_WSC2; <sup>i</sup> LV3\_SC2 = LV3\_WSC2; <sup>j</sup> LV4\_SC2 < LV4\_WSC2; <sup>k</sup> LV4\_SC2 > LV4\_WSC2; <sup>l</sup> LV4\_SC2 = LV4\_WSC2.

**Table 8.** The results of the Wilcoxon signed-rank test reveal a significant relationship between the performance of SC and non-SC scenarios.

Test Statistics <sup>a</sup>				
	Lv1_SC2– Lv1_WSC2	LV2_SC2– LV2_WSC2	LV3_SC2– LV3_WSC2	LV4_SC2– LV4_WSC2
Z	−3.920 <sup>b</sup>	−3.920 <sup>b</sup>	−3.920 <sup>b</sup>	−3.920 <sup>b</sup>
Asymp. Sig., <i>p</i> (2-tailed)	0.000	0.000	0.000	0.000

Note: SC = scenarios with solar chimney, WSC = scenarios without solar chimney; <sup>a</sup> Wilcoxon signed-rank test; <sup>b</sup> based on negative ranks.

Figures 11 and 12 compare the performance of the SC with and without the assistance of a ceiling fan. The scenarios with ceiling fans not only demonstrated higher wind velocities of up to 1.5 m/s within the room, but also encouraged a greater inflow of air from the inlet aperture (Sensor A1C1), although the degree of impact varied depending on the altitude of the level from the ground. However, the introduction of the SC in Scenarios 3 and 4 additionally encouraged higher wind velocities within the SC (Sensor A1C7), implying that the Bernoulli principle was in effect. The use of ceiling fans alone to assist with natural ventilation had a less pronounced effect on air convection that would have encouraged the SC effect and, thus, better ventilation.

We determined an R-squared value of 0.4687 for the scenarios with the SC, suggesting that the induction of the SC effect is able to improve natural airflow by over 45% in an apartment unit in Malaysia. However, the absence of a ceiling fan negatively affected the performance of the SC (see Figure 11), with the exception of Level 2, in which several sensors closer to the windward aperture still generated a positive effect, and a room with neither a ceiling fan nor SC performed better than an SC-only room.

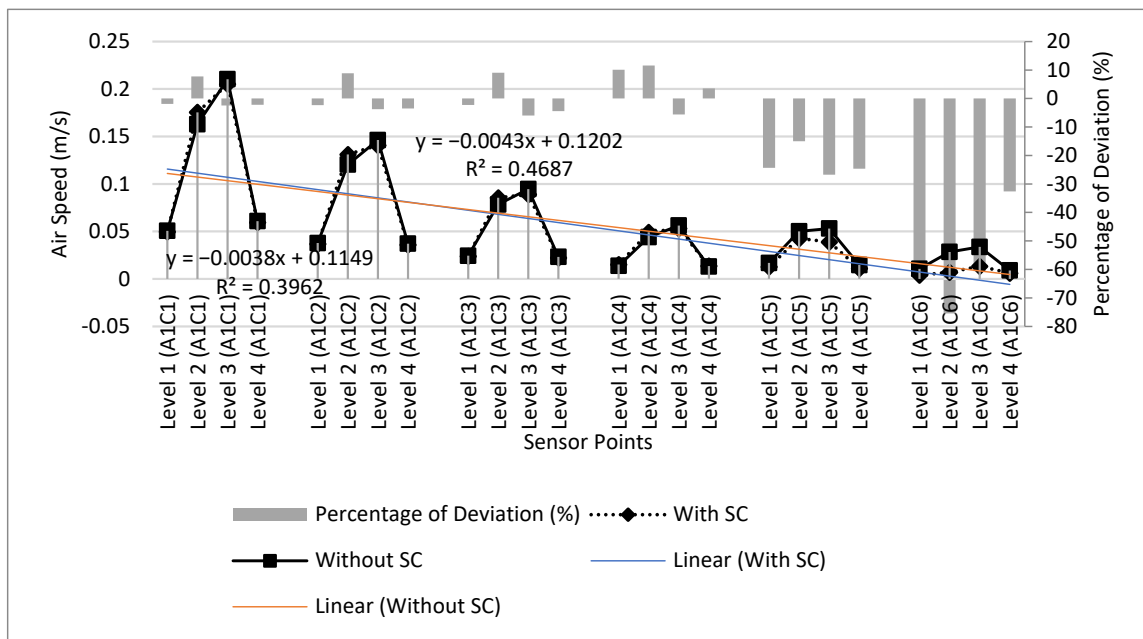


Figure 11. Comparison of indoor air speed between a room with an SC and a room without an SC, without the assistance of a ceiling fan.

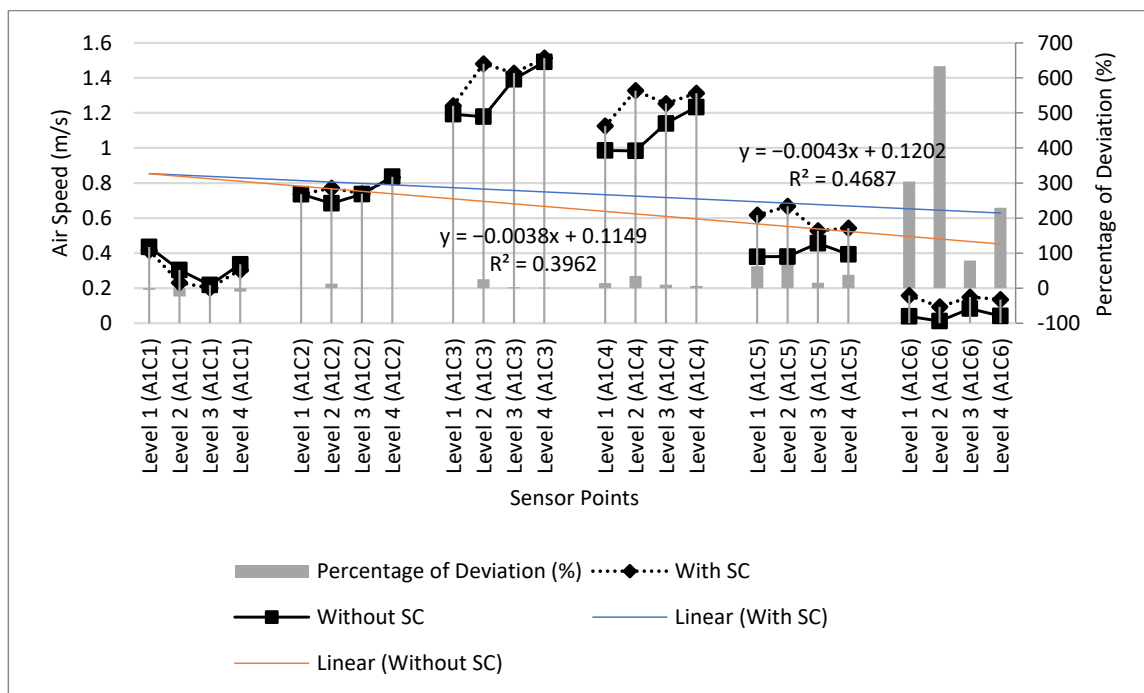


Figure 12. Comparison of indoor air speed between a room with an SC and a room without an SC, with the assistance of a ceiling fan.

When complemented with a ceiling fan, the overall resultant air speed improved in a parabolic pattern, where areas closest to the fan exhibited the greatest improvement. The use of a ceiling fan alone returned an R-squared value of 0.3962, making it a slightly less reliable indicator of fresh air exchange.

However, the impact of an SC varied with the altitude of the simulated level from the ground, regardless of the presence of a ceiling fan. The effect was most pronounced at Level 2, which is the level immediately above Level 1 (ground level). When an SC was

used in conjunction with a ceiling fan, the overall wind velocity within the room improved, achieving air speeds of approximately 1.3–1.5 m/s near the ceiling fan (see Figure 12). Areas further from the windward aperture exhibited greater improvements, suggesting a better distribution of natural ventilation throughout the room.

#### 4. Conclusions and Recommendations

This paper determined that the introduction of a solar chimney, or the elements that induce its effect, is an effective passive means of improving natural ventilation in public housing in tropical climates. Overall, this study proved that the solar chimney—especially when used in conjunction with a ceiling fan—is a viable and effective means of improving natural ventilation in tropical public housing via enhanced ACH, achieved by promoting natural air-flow rates within and through an indoor space. The combination of the solar chimney and ceiling fan achieved a 45% improvement in indoor air velocity and a minimum ACH of 92.42 in the case study room, which is well above the minimum recommended ACH for hospitals. Having thus virtually ascertained that its incorporation demonstrates a statistically significant improvement over current layout design practices, we may devise further strategies to enable the solar chimney effect through innovations in construction material choices and spatial arrangements.

However, the empirical simulations assume that the space is capable of cross-ventilation, and it must be noted that apartment layouts may result in spaces that enjoy only single-sided ventilation, so the solar chimney should be positioned for maximum impact. Further studies would be required to extrapolate these findings for other building typologies and climates. Other factors that affect natural ventilation—such as fenestration design and positioning, opening altitude, and the presence of adjacent structures—also merit consideration for future policymaking exercises. Future research into the correlations between air velocity, ACH, and indoor air quality (IAQ) merits consideration.

This paper ultimately proposes several recommendations as follows:

##### 4.1. Improve Thermo-Syphonic Effect

The layout of typical high-rise residential units can be improved to induce the thermo-syphonic effect in addition to cross-ventilation. The positions and dimensions of the apertures should be given due consideration. Scenarios 3 and 4 allowed for a 0.16 m high gap lengthwise across the external wall of the intended solar chimney (i.e., the bathroom), although further simulations may discover alternate dimensions. The simulated aperture, when combined with a ceiling fan, was able to improve air velocity by over 45%. Generally, the inlet of the solar chimney should be lower than the outlet.

The passiveness of the solar chimney makes it a cost-effective option for public housing, which tends to be constructed on a limited budget. Instead of a monofunctional solar chimney, natural ventilation may be optimised through strategic spatial planning and modifications to the external wall's materials or design, using basic construction techniques that are readily available on the market. This would make its adoption more cost-effective.

The solar chimney concept may be implemented using spaces meant for transitions or temporary occupation, in order to avoid prolonged negative user comfort within the solar chimney space. Possible innovations include permanent, built-in openings in intermediate spatial dividers, such as fixed louvres at the bottom sections of doors or walls. These should be weighed against user privacy and noise insulation needs.

##### 4.2. Considerations of SC External Wall Materials

Although this study assumes that the external wall of the designated solar chimney is made of brick, which is a common practice in Malaysia, alternative materials with higher thermal conductivity may be considered for better performance. Materials with higher thermal conductivity (such as metal), or those with higher thermal mass (such as concrete), may increase the effectiveness of the SC. However, designers will also need to consider strategies to mitigate radiant heat transfer into habitable spaces.



Alternatively, a secondary façade skin, distanced from the external walls and windows of the building, may serve to induce the solar chimney effect without necessitating significant modifications to internal layouts and specifications.

**Author Contributions:** Conceptualization, P.C.L. and G.H.T.L.; Data curation, N.E.H.A.; Formal analysis, G.H.T.L.; Investigation, P.C.L.; Methodology, S.B.A. and Y.L.L.; Project administration, M.H.A.; Resources, N.E.H.A., G.H.T.L. and Y.L.L.; Software, S.B.A. and Y.L.L.; Supervision, P.C.L. and M.H.A.; Validation, N.E.H.A., G.H.T.L., Y.L.L. and M.H.A.; Visualization, P.C.L. and N.E.H.A.; Writing—original draft, P.C.L.; Writing—review & editing, S.B.A. All authors have read and agreed to the published version of the manuscript.

**Funding:** This research publication was supported by UTM Research University Grant (Tier 2) No. Q.J130000.2652.16J79.

**Institutional Review Board Statement:** Not applicable.

**Informed Consent Statement:** Not applicable.

**Data Availability Statement:** Not applicable.

**Acknowledgments:** The authors wish to deliver appreciation to UTM Research University Grant (GUP) for the funding entitled “Optimization of Natural Ventilation with Solar Chimney for Single Storey Terrace House in Tropical Climate” (Q.J130000.2652.16J79), Building Science Laboratory of UTM Faculty of Built Environment and Surveying for the courtesy providing measurement instrument as well as to Bong Ted Shoon for allowing field measurement for air velocity of existing multi-storey case study house at Pulai Flora, Skudai, Johor Malaysia. We also thanks for the 2 anonymous reviewers for their constructive comments and suggestions.

**Conflicts of Interest:** The authors declare no conflict of interest. The funders had no role in the design of the study; in the collection, analyses, or interpretation of data; in the writing of the manuscript, or in the decision to publish the results.

## References

1. Cao, Y.; Pourhedayat, S.; Dizaji, H.S.; Wae-hayee, M. A Comprehensive Optimization of Phase Change Material in Hybrid Application with Solar Chimney and Photovoltaic Panel for Simultaneous Power Production and Air Ventilation. *Build. Environ.* **2021**, *197*, 107833. [CrossRef]
2. Blinc, A.; Buturović Ponikvar, J.; Fras, Z. Airborne Spread of SARS-CoV-2—A Commentary by the Division of Internal Medicine, University Medical Centre Ljubljana. *Slov. Med. J.* **2022**, *1–7*. [CrossRef]
3. McDowall, R. Ventilation and Indoor Air Quality. In *Fundamentals of HVAC Systems*; Elsevier: Amsterdam, The Netherlands, 2007; pp. 45–61. ISBN 978-0-12-373998-8.
4. Ching, J.; Kajino, M. Rethinking Air Quality and Climate Change after COVID-19. *Int. J. Environ. Res. Public Health* **2020**, *17*, 5167. [CrossRef] [PubMed]
5. Kwok, H.H.L.; Cheng, J.C.P.; Li, A.T.Y.; Tong, J.C.K.; Lau, A.K.H. Impact of Shaft Design to Thermal Comfort and Indoor Air Quality of Floors Using BIM Technology. *J. Build. Eng.* **2022**, *51*, 104326. [CrossRef]
6. ANSI/ASHRAE Standards and Guidelines to Address COVID-19; ASHRAE, 27 February 2020. Available online: <https://www.ashrae.org/about/news/2020/ashrae-resources-available-to-address-covid-19-concerns> (accessed on 10 April 2022).
7. Persily, A. Challenges in Developing Ventilation and Indoor Air Quality Standards: The Story of ASHRAE Standard 62. *Build. Environ.* **2015**, *91*, 61–69. [CrossRef]
8. Allen, J.G.; Ibrahim, A.M. Indoor Air Changes and Potential Implications for SARS-CoV-2 Transmission. *JAMA* **2021**, *325*, 2112. [CrossRef]
9. Fisk, W.J. The Ventilation Problem in Schools: Literature Review. *Indoor Air* **2017**, *27*, 1039–1051. [CrossRef]
10. *Selangor Uniform Building by-Laws 1986 (Amendment 2012)*; MDC Publishers Sdn Bhd: Kuala Lumpur, Malaysia, 2012; ISBN 978-967-70-1492-3.
11. Du, L.; Ping, L.; Yongming, C. Study and Analysis of Air Flow Characteristics in Trombe Wall. *Renew. Energy* **2020**, *162*, 234–241. [CrossRef]
12. Chaturvedi, S.K.; Mohieldin, T.O.; Huang, G.C. Mixed Laminar Convection in Trombe Wall Channels. *J. Sol. Energy Eng.* **1988**, *110*, 31–37. [CrossRef]
13. Bojić, M.; Johannes, K.; Kuznik, F. Optimizing Energy and Environmental Performance of Passive Trombe Wall. *Energy Build.* **2014**, *70*, 279–286. [CrossRef]
14. Gan, G. Simulation of Buoyancy-Induced Flow in Open Cavities for Natural Ventilation. *Energy Build.* **2006**, *38*, 410–420. [CrossRef]

15. Tan, A.Y.K.; Wong, N.H. Natural Ventilation Performance of Classroom with Solar Chimney System. *Energy Build.* **2012**, *53*, 19–27. [[CrossRef](#)]
16. Chung, L.P.; Ahmad, M.H.; Ossen, D.R.; Hamid, M. Effective Solar Chimney Cross Section Ventilation Performance in Malaysia Terraced House. *Procedia Soc. Behav. Sci.* **2015**, *179*, 276–289. [[CrossRef](#)]
17. Hassanein, S.A.; Abdel-Fadeel, W.A. Improvement of Natural Ventilation in Building Using Multi Solar Chimneys at Different Directions. *JES J. Eng. Sci.* **2012**, *40*, 1661–1677. [[CrossRef](#)]
18. Gong, N.; Tham, K.W.; Melikov, A.K.; Wyon, D.P.; Sekhar, S.C.; Cheong, K.W. The Acceptable Air Velocity Range for Local Air Movement in the Tropics. *HVACR Res.* **2006**, *12*, 1065–1076. [[CrossRef](#)]
19. Roghanchi, P.; Kocsis, K.C.; Sunkpal, M. Sensitivity Analysis of the Effect of Airflow Velocity on the Thermal Comfort in Underground Mines. *J. Sustain. Min.* **2016**, *15*, 175–180. [[CrossRef](#)]
20. Xie, C. Interactive Heat Transfer Simulations for Everyone. *Phys. Teach.* **2012**, *50*, 237–240. [[CrossRef](#)]
21. Punin, W.; Maneewan, S.; Punlek, C. Heat Transfer Characteristics of a Thermoelectric Power Generator System for Low-Grade Waste Heat Recovery from the Sugar Industry. *Heat Mass Transf.* **2019**, *55*, 979–991. [[CrossRef](#)]
22. Massaro, A.; Galiano, A.; Meuli, G.; Massari, S.F. Overview and Application of Enabling Technologies Oriented on Energy Routing Monitoring, on Network Installation and on Predictive Maintenance. *Int. J. Artif. Intell. Appl.* **2018**, *9*, 1–20. [[CrossRef](#)]
23. Navarro, J.A.A.; Téllez, M.C.; Martínez, M.A.R.; Silvar, G.P.; Tejada, F.C.M. Computational Thermal Analysis of a Double Slope Solar Still Using Energy2D. *Desalin. Water Treat.* **2019**, *151*, 26–33. [[CrossRef](#)]
24. Joshua, A.; Lim, Y.-W. Daylighting and Lighting Energy Saving in South-Oriented Open-Plan Office with Light Shelf in the Tropics. *Clin. Med.* **2020**, *7*, 22.
25. Royapoor, M.; Roskilly, T. Building Model Calibration Using Energy and Environmental Data. *Energy Build.* **2015**, *94*, 109–120. [[CrossRef](#)]
26. Bughrara, K.S.M.; Durmu, Z. Effect of Intervention Strategies on Seasonal Thermal Comfort Conditions in a Historic Mosque in the Mediterranean Climate. In Proceedings of the 3rd International Conference on Energy Efficiency in Historic Buildings (EEHB2018), Visby, Sweden, 26–27 September 2018; Volume 9.
27. AgriMetSoft Correlation Coefficient. Available online: <https://agrimetsoft.com/calculators/correlation%20coefficient> (accessed on 10 May 2022).